

Waveform Moment Analysis in Psychophysiological Research

John T. Cacioppo and Donald D. Dorfman
University of Iowa

Quantitative representations of nonnegative bounded waveforms have traditionally been insensitive to substantive features of the topography of those waveforms. This is an important class of waveforms in psychophysiology, ranging from the integrated electromyographic response in the time domain to the amplitude distribution of the electroencephalogram to the power spectrum of the various bioelectric signals. In the present article, we outline a quantitative representation of nonnegative bounded waveforms predicated on the moments of the waveform in a given domain: The first moment provides the basis for a measure of central tendency, the higher order even moments provide the basis for a multidimensional indicant of dispersion about a specified reference point (e.g., about the first moment), and the higher order odd moments provide the basis for a multidimensional indicant of asymmetry about the specified reference point. We show that these indicants provide shape descriptions of nonnegative bounded waveforms and present evidence suggesting that moment-based indicants offer a mathematically rigorous yet easily interpretable summary of bioelectric signals in the time, amplitude, and frequency domains. Advantages and limitations of using the moment-based indicants to compare responses are discussed.

A quantity of data which by its mere bulk may be incapable of entering the mind is to be replaced by relatively few quantities which shall adequately represent the whole, or which, in other words, shall contain as much as possible, ideally the whole, of the relevant information contained in the original data. (Fisher, 1922, p. 309)

As Fisher (1922) noted, a general problem in statistics is summarizing complex data in a manner that minimizes the loss of information while it renders their significance comprehensible. Data may take various forms, ranging from amplitudes across time that constitute a "response" to the collection of indexes of responses across many trials, conditions, and subjects. We are concerned here with the problem of deriving a useful and interpretable summary of waveforms that are nonnegative and bounded. More specifically, let $f(x)$ denote a waveform defined on x . We are interested in waveforms that have the following two general characteristics: (a) $f(x)$ and x are bounded, and (b) $f(x) \geq 0$. For responses generated by a living organism, time is necessarily bounded. Moreover, in laboratory practice, responses generated by living organisms are inevitably bounded in amplitude as well as time. Although physiological responses

characterized by nonnegative amplitudes across time are an important class of bioelectric events, it should be noted that all psychophysiological responses are nonnegative and bounded in the amplitude and frequency domains. Hence, the analysis of waveforms having the two characteristics above should be of some general interest. We refer to waveforms that are nonnegative and bounded as *NB waveforms*.

Overview

In the present article, we extend earlier work on the theoretical and empirical utility of indicants based on the moments of an NB waveform.¹ The initial set of indicants we used—standard measures of mean, variance, skewness, and kurtosis in the time and amplitude domains—has proven capable of distinguishing between unique NB waveforms (Cacioppo, Marshall-Goodell, & Dorfman, 1983) and integrated electromyographic (IEMG) responses resulting from various isometric (Cacioppo et al., 1983; Cacioppo, Petty, & Marshall-Goodell, 1984) and mild isotonic (Grabiner, Andonian, Regnier, & Harding, 1984) muscle contraction tasks. Moreover, recent research in which IEMG activity has been recorded over superficial muscle regions in the human face and forearm has demonstrated its empirical and theoretical utility in studies of information processing (Cacioppo, Petty, & Morris, 1985) and of affective imagery (Cacioppo et al., 1984).

These indicants have also been used in research on the electroencephalogram (EEG) to characterize the shape of the power

This research was supported by National Science Foundation Grants BNS-8217096 and BNS-8444909.

We thank Bernard Saltzberg for his helpful discussion; Robert J. Cacioppo and an anonymous reviewer for their comments on an earlier draft of this article; Jennifer Dorfman and Beverly Marshall-Goodell for their assistance in data collection and reduction; and Louis Tassinary, Stacey Siegel, Fuchih Chen, and Beverly Marshall-Goodell for programming various versions of WAMA (Waveform Moments Analysis).

A user-friendly computer program to illustrate the calculation of moment-based indicants is available on request. Versions of the program are written in BASIC to execute on the Apple II Plus, Apple IIe, or Apple Macintosh or in ASYST to execute on the IBM-PC and compatibles.

Correspondence concerning this article should be addressed to John T. Cacioppo, Department of Psychology, University of Iowa, Iowa City, Iowa 52242.

¹ The mathematical term *moment* has its origin in physics (mechanics), in which the first moment of force is defined as a measure of force with respect to the tendency of the force to produce rotation (Peatman, 1947, p. 150). If one converts a mass distribution to a unit mass, the first and second moments about the origin in mechanics are the center of gravity and the square of the radius of gyration, respectively, and the square of the radius of gyration is equivalent to the moment of inertia about the origin (Bracewell, 1978).

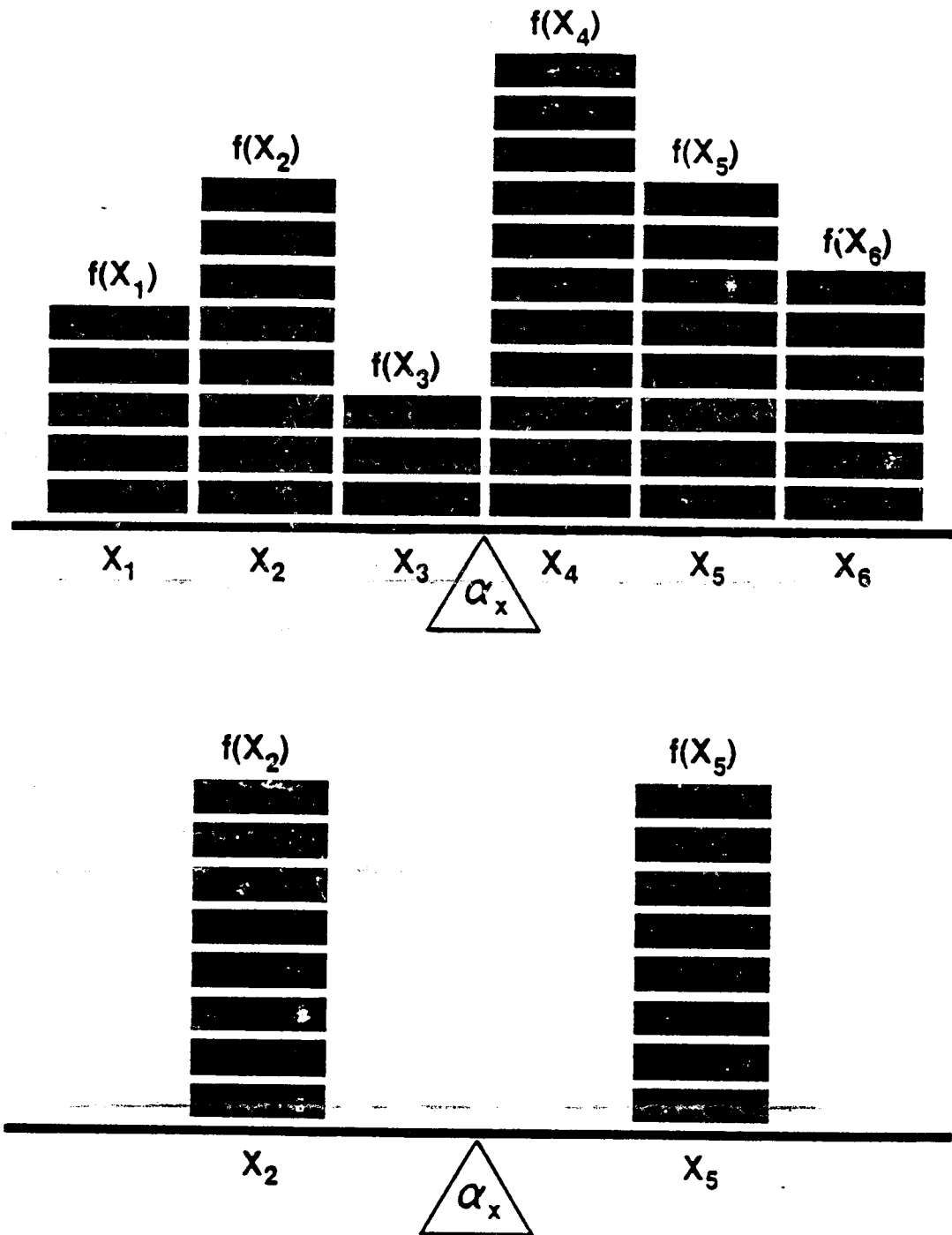


Figure 1. Top: Stacks of bricks of mass $f(x_i)$ applied simultaneously at positions x_i along a beam, which is supported by a fulcrum at α_x . Bottom: Two stacks of bricks of equal mass and positioned equidistant from but on opposite sides of α_x .

spectral density (PSD), that is, the EEG expressed in the frequency domain. Hjorth (1970, 1973, 1975) has characterized the EEG in terms of three parameters: activity, mobility, and complexity. *Activity* refers to the area of the two-sided PSD; *mobility* refers to the standard deviation of the two-sided PSD normalized to an area of one; and *complexity* refers to its kurtosis. The two-sided PSD is always symmetrical about zero, and

therefore, the mean and skewness are necessarily zero and are not computed. In fact, symmetry implies a value of zero for all the odd moments. Saltzberg, Burton, Barlow, and Burch (1985) characterized the physically meaningful one-sided PSD (normalized to an area of one) by its mean, variance, skewness, and kurtosis. They estimated these shape descriptors with a robust computer-efficient procedure that uses the autocorrelation

function. Their innovative method can also be used to estimate even moments of the two-sided PSD.

In the amplitude domain, Bronzino, Kelly, Cordova, Oley, and Morgane (1981) proposed the use of the variance, skewness, and kurtosis as shape descriptors of the distribution of EEG amplitudes. They did not consider the mean, arguing that changes in the mean are of technical origin (e.g., amplifier drift). They showed that these indicants are capable of quantifying alterations in the electrical processes brought about by pharmacological manipulations.

The major goals of the present article are (a) to describe possible applications of such moment-based indicants as mean, variance, skewness, and kurtosis for describing NB waveforms in the time domain, amplitude domain, and frequency domain and (b) to present a general framework for a moment-based analysis that yields a set of multidimensional indicants subsuming the above-mentioned classical descriptors. A general framework for moment-based indicants may offer investigators more flexibility and more options in gaining information from moment-based probes of NB waveforms. In the case of NB waveforms, all moments exist, and the moments fully characterize the waveform (see Rao, 1965). To facilitate insight, we begin by discussing rudimentary features of the present analysis, using a simple example from physics of force applied simultaneously at various distances along a lever (see Figure 1). We then turn to summarizing responses that constitute NB waveforms in the (a) time domain, such as IEMG responses; (b) amplitude domain, such as IEMG responses, electroencephalographic (EEG) activity, and event-related potentials; and (c) frequency domain, such as the power spectrum of the EEG and of the electromyogram (EMG).

Force and Distance: A Tutorial

For purposes of illustration, view the data depicted in Figure 1 as bricks stacked atop a beam with a fulcrum placed at an arbitrary position, α_x . The distribution of bricks atop the beam can be viewed as an example of an NB waveform. By assuming that gravity is constant, we find that the force exerted at each position, x_i , along the beam equals the mass, $f(x_i)$, times a constant. Hence, the top panel of Figure 1 can be viewed as depicting points of force ($x_i, f(x_i)$), where x_i signifies some position along the beam and $f(x_i)$ is proportional to the force exerted at location x_i along the beam.

The moments of this distribution of bricks provide the basis for differentiating this from alternative distributions of bricks that might be placed atop the beam as well as for identifying the manner in which this and an alternative distribution of bricks differ. To begin, notice that the tendency for any given stack of bricks to produce rotation of the beam is given by the expression $|x_i - \alpha_x|f(x_i)$, indicating that the tendency for any given stack of bricks to induce rotation about the fulcrum is proportional to (a) the distance from the fulcrum at which the stack of bricks is positioned (i.e., $|x_i - \alpha_x|$) and (b) the mass of the stack of bricks (i.e., $f(x_i)$). If N stacks of bricks are simultaneously placed atop the beam at positions x_1, x_2, \dots, x_N , then the total tendency of this particular distribution of bricks to induce rotation is given by

$$\sum_{x_i > \alpha_x} |x_i - \alpha_x|f(x_i) - \sum_{x_i < \alpha_x} |x_i - \alpha_x|f(x_i),$$

which equals

$$\sum_{i=1}^N (x_i - \alpha_x)f(x_i) = \mu'_{1;x}, \quad (1)$$

the first moment about the arbitrary position, α_x , of the fulcrum. It is worth noting that if

$$\sum_{i=1}^N (x_i - \alpha_x)f(x_i)$$

is negative, then there will be a counterclockwise rotation about the fulcrum; if the quantity is positive, then there will be a clockwise rotation about the fulcrum. If

$$\sum_{i=1}^N (x_i - \alpha_x)f(x_i) = 0,$$

then the distribution of bricks is at equilibrium. In that case,

$$\sum_{i=1}^N x_i f(x_i) = \alpha_x \sum_{i=1}^N f(x_i).$$

Thus, the point at which the fulcrum will balance the beam is

$$\alpha_x = \frac{\sum_{i=1}^N x_i f(x_i)}{\sum_{i=1}^N f(x_i)},$$

which is the abscissa of the center of gravity of the distribution of bricks. Note that the abscissa of the center of gravity is equivalent to the first moment about the origin of the distribution of bricks converted to a unit mass.

In the general case, the k th moment of this distribution of bricks about α_x is

$$\mu'_{k;x} = \sum_{i=1}^N (x_i - \alpha_x)^k f(x_i). \quad (2)$$

Let us convert the distribution of mass to a unit mass by dividing the mass, $f(x_i)$, of each stack of bricks by $\sum_{i=1}^N f(x_i)$. Equating the waveforms with respect to the total amplitude by expressing each amplitude, $f(x_i)$, as a proportion of the total amplitude, $\sum_{i=1}^N f(x_i)$, provides a size-independent measure of the shape of the waveform (i.e., total mass, defined as $\sum_{i=1}^N f(x_i)$) and facilitates comparison of the shapes of NB waveforms, or in terms of our example, the shapes of distributions of bricks atop a beam. Before we elaborate on this latter point, note that this transformation converts the distribution to a probability distribution, where the probability of the event (x_i) is

$$P(\{x_i\}) = \frac{f(x_i)}{\sum_{i=1}^N f(x_i)}.$$

Technically speaking, we have converted the weight distribution

depicted in Figure 1 to a probability density function. (See Hoel, Port. & Stone, 1971, for a discussion of discrete and continuous probability density functions.)

Now that we have converted the mass distribution to a probability distribution, we see that the abscissa of the center of gravity

$$\frac{\sum_{i=1}^N x_i f(x_i)}{\sum_{i=1}^N f(x_i)} = \mu_x$$

is an arithmetic mean. Also, if we let $k = 2$, we see that

$$\frac{\sum_{i=1}^N (x_i - \mu_x)^2 f(x_i)}{\sum_{i=1}^N f(x_i)} = \sigma_x^2$$

is the variance of the x_i 's. Moreover, for $k = 3$ and $\alpha_x = \mu_x$,

$$\frac{\sum_{i=1}^N \left(\frac{x_i - \mu_x}{\sigma_x} \right)^3 f(x_i)}{\sum_{i=1}^N f(x_i)} = \gamma_1$$

is a standard measure of skewness, γ_1 , (see Kendall & Stuart, 1963). For $k = 4$ and $\alpha_x = \mu_x$,

$$\frac{\sum_{i=1}^N \left(\frac{x_i - \mu_x}{\sigma_x} \right)^4 f(x_i)}{\sum_{i=1}^N f(x_i)} = \gamma_2 + 3 = \beta_2,$$

a standard measure of kurtosis (see Kendall & Stuart, 1963). For a normal distribution, $\beta_2 = 3$. Historically, kurtosis has been defined as peakedness (see Chissom, 1970; Dariington, 1970; Hildebrand, 1971; Moors, 1986, for a lively discussion of the meaning of kurtosis), but as should soon become clear, the standard measure of kurtosis is in fact a measure of dispersion.

Characterization of a Distribution by Its Moments

In the case of NB waveforms, it is not difficult to show that all the moments exist and, furthermore, that the NB waveform can be uniquely characterized by its moments and its total mass. Some investigators characterize a waveform by its Fourier transform. In the case of NB waveforms, it can be shown that the moments and the total mass of the NB waveform uniquely and fully characterize the Fourier transform (Feller, 1966; Rao, 1965). Moreover, if the moments of two equal-mass NB waveforms are similar, the waveforms are similar (Feller, 1966; Rao, 1965; cf. Kendall & Stuart, 1963).

Furthermore, the sequence of moments about α_x obtained when k is even ($k = 2, 4, 6, \dots$) can be used to gauge the dispersion of the distribution of bricks about α_x , and the sequence of moments about α_x obtained when k is odd ($k = 1, 3, 5, 7, \dots$) can be used to gauge the asymmetry of the distribution of bricks about α_x . In the following sections, we work with Figure 1 and Equation 2 to illustrate that (a) the odd moments are zero if and

only if the NB waveform is symmetric about α_x and (b) the even moments yield a sequence of indicants of dispersion of the NB waveform about α_x .

Asymmetry: Notice that if we place two stacks of bricks of the same height at equal distances from but on opposite sides of α_x , we obtain a perfect balance, that is, no net rotation about α_x (see Figure 1, bottom panel). We obtain a balance because the first odd moment about α_x is zero since

$$|x_2 - \alpha_x| f(x_2) = |x_3 - \alpha_x| f(x_3).$$

In fact, all the odd moments are zero in the case illustrated in the bottom panel of Figure 1. If we inspect Equation 2, the equation for the moments, we see that the co-stacks equidistant from but on opposite sides of α_x have equal and opposite effects on all the odd moments, so that the net effect is that all the odd moments about α_x are zero in this case. For instance, let $\{(x_i, f(x_i); x_i^*, f(x_i^*))\}$ be a pair of stacks of the same height equidistant from α_x where $x_i < \alpha_x < x_i^*$. Clearly,

$$|x_i - \alpha_x| = |x_i^* - \alpha_x|,$$

so that

$$-(x_i - \alpha_x) = (x_i^* - \alpha_x)$$

because $|y| = -y$ when $y < 0$. Therefore,

$$(-1)^k (x_i - \alpha_x)^k = (x_i^* - \alpha_x)^k.$$

In view of the fact that $(-1)^k = -1$ for k odd,

$$-(x_i - \alpha_x)^k = (x_i^* - \alpha_x)^k.$$

Thus, each member of a pair of co-stacks has equal and opposite effects. But from Equation 2, we know that

$$\begin{aligned} \mu_{k;x} &= \sum_{i=1}^{N/2} (x_i - \alpha_x)^k f(x_i) + \sum_{i=1}^{N/2} (x_i^* - \alpha_x)^k f(x_i^*) \\ &= \sum_{i=1}^{N/2} (x_i - \alpha_x)^k f(x_i) - \sum_{i=1}^{N/2} (x_i - \alpha_x)^k f(x_i) \\ &= 0, \end{aligned}$$

because $-(x_i - \alpha_x)^k = (x_i^* - \alpha_x)^k$ and $f(x_i) = f(x_i^*)$. Thus, if we construct a symmetric distribution of bricks about α_x , all the odd moments about α_x turn out to be zero. If one or more of the odd moments about α_x are not zero, the distribution of bricks is asymmetric about α_x . In short, the odd moments about α_x provide a multidimensional gauge of asymmetry about α_x .

Note that this multidimensional gauge provides information about the direction as well as the extent of asymmetry about α_x . If

$$-\sum_{x_i < \alpha_x} (x_i - \alpha_x)^k f(x_i) < \sum_{x_i > \alpha_x} (x_i - \alpha_x)^k f(x_i),$$

then the k th odd moment is positive, so that we have a k th-power positive asymmetry. If

$$-\sum_{x_i < \alpha_x} (x_i - \alpha_x)^k f(x_i) > \sum_{x_i > \alpha_x} (x_i - \alpha_x)^k f(x_i),$$

then the k th odd moment is negative, so that we have a k th-power negative asymmetry.

The order of the moment is also significant. Traditionally, only indexes of asymmetry for $k = 3$ have been considered when α_x is the arithmetic mean—a tradition that holds for previous analyses of the asymmetry of psychophysiological waveforms as well (e.g., Bronzino et al., 1981; Cacioppo et al., 1983; Saltzberg et al., 1985). But with the ready availability of the high-speed digital computer, one might profitably compute higher order indicants of asymmetry, thereby providing a more complete summary of the asymmetries in an NB waveform. We return to a fuller discussion of the interpretation of these higher order indicants in a subsequent section, but we first address the basis for using the even moments to index the dispersion of NB waveforms.

Dispersion. Because $(x_i - \alpha_x)^k > 0$ for $x_i \neq \alpha_x$ and k even,

$$(x_i - \alpha_x)^k f(x_i) > 0$$

when dealing with NB waveforms. Hence, for k even,

$$\sum_{i=1}^N (x_i - \alpha_x)^k f(x_i) > 0.$$

This means that the even moments are always positive except, of course, for the case in which $f(x_i) > 0$ for $x_i = \alpha_x$ and $f(x_i) = 0$ for all x_i not equal to α_x . In this case,

$$\sum_{i=1}^N (x_i - \alpha_x)^k f(x_i) = 0.$$

Moreover, inspection of Equation 2 reveals that the even moments are sensitive to the absolute deviations of the locations, x_i , of the stacks of bricks from α_x . For instance, in the case of even moments, in contrast to the odd moments, identical stacks of bricks placed equidistant from but on opposite sides of α_x (see Figure 1) do not cancel the effects of each. For even moments, the effects

$$(x_i - \alpha_x)^k f(x_i)$$

sum. The greater the distance of the stacks from α_x , the greater the impact on the sum

$$\sum_{i=1}^N (x_i - \alpha_x)^k f(x_i).$$

Thus, the dispersion of the stacks of bricks about the reference point α_x can be gauged by using the even moments, and these moments provide a mathematically rigorous manner of comparing the dispersion of various stacks of bricks when each stack is expressed in unit mass.

Weighted Euclidean Distances: The Interpretation of Moments

For fully understanding the moments, it is useful to think of

$$(x_i - \alpha_x)^k f(x_i)$$

as a weighted Euclidean distance. If k is even, then

$$(x_i - \alpha_x)^k = |x_i - \alpha_x|^k$$

because $(x_i - \alpha_x)^k$ is nonnegative. Notice that $|x_i - \alpha_x|$ is the standard Euclidean distance between x_i and α_x on the beam. Recall that if x_1 and x_2 are two points on a line, such as a beam,

the Euclidean distance between those two points is the number $|x_1 - x_2|$. It is also the case that for k even,

$$(x_i - \alpha_x)^k f(x_i) = |x_i - \alpha_x| |x_i - \alpha_x|^{k-1} f(x_i).$$

Therefore, for k even, we can usefully consider $(x_i - \alpha_x)^k f(x_i)$ as the Euclidean distance between x_i and α_x , $|x_i - \alpha_x|$, weighted by the factor $|x_i - \alpha_x|^{k-1} f(x_i)$. In short,

$$(x_i - \alpha_x)^k f(x_i)$$

is a weighted Euclidean distance when k is even.

Now consider the odd moments. For k odd,

$$\begin{aligned} \mu'_{k;x} &= \sum_{x_i > \alpha_x} (x_i - \alpha_x)^k f(x_i) + \sum_{x_i < \alpha_x} (x_i - \alpha_x)^k f(x_i) \\ &= \sum_{x_i > \alpha_x} |x_i - \alpha_x|^k f(x_i) - \sum_{x_i < \alpha_x} |x_i - \alpha_x|^k f(x_i) \end{aligned}$$

because $|(x_i - \alpha_x)| = -(x_i - \alpha_x)$ for $(x_i - \alpha_x) < 0$ and $|(x_i - \alpha_x)| = (x_i - \alpha_x)$ for $(x_i - \alpha_x) \geq 0$. Hence,

$$\begin{aligned} \mu'_{k;x} &= \sum_{x_i > \alpha_x} |x_i - \alpha_x| |x_i - \alpha_x|^{k-1} f(x_i) \\ &\quad - \sum_{x_i < \alpha_x} |x_i - \alpha_x| |x_i - \alpha_x|^{k-1} f(x_i). \end{aligned}$$

Thus, the odd moments can be viewed as the difference between two sums of weighted Euclidean distances: one sum generated from the set of x_i s to the right of α_x on the beam ($x_i > \alpha_x$) and the second sum generated from the set of x_i s to the left of α_x on the beam ($x_i < \alpha_x$). To appreciate the role of the weight

$$|x_i - \alpha_x|^{k-1} f(x_i),$$

let k increase. When $k = 1$, the weight assigned to $|x_i - \alpha_x|$ is

$$|x_i - \alpha_x|^0 f(x_i) = f(x_i).$$

When $k > 1$, the weight

$$|x_i - \alpha_x|^{k-1} f(x_i)$$

(a) goes to zero as k goes to infinity for $|x_i - \alpha_x| < 1$, (b) equals $f(x_i)$ for all k when $|x_i - \alpha_x| = 1$, and (c) goes to infinity when k goes to infinity for $|x_i - \alpha_x| > 1$. Figure 2 is a pictorial representation of these effects under the simplifying assumption that $f(x_i) = 1$.

This weighting function has the effect of providing a correlated but unique probe of asymmetry for each odd k and a correlated but unique probe of dispersion for each even k . These probes are interesting in that each probe—that is, each moment-based indicant—uses all the data, but as k increases, large deviations play an increasingly large role. Finally, it should be reemphasized that two distributions, such as two distributions of bricks atop a beam, are identical if and only if all the moments of asymmetry and dispersion are equal and they have the same total mass (Feller, 1966; Rao, 1965).

Multidimensional Indicants

To summarize thus far, the first n odd moments provide the basis for an n -dimensional indicant of asymmetry of the distribution of x_i about α_x —that is, a vector-valued measure of the

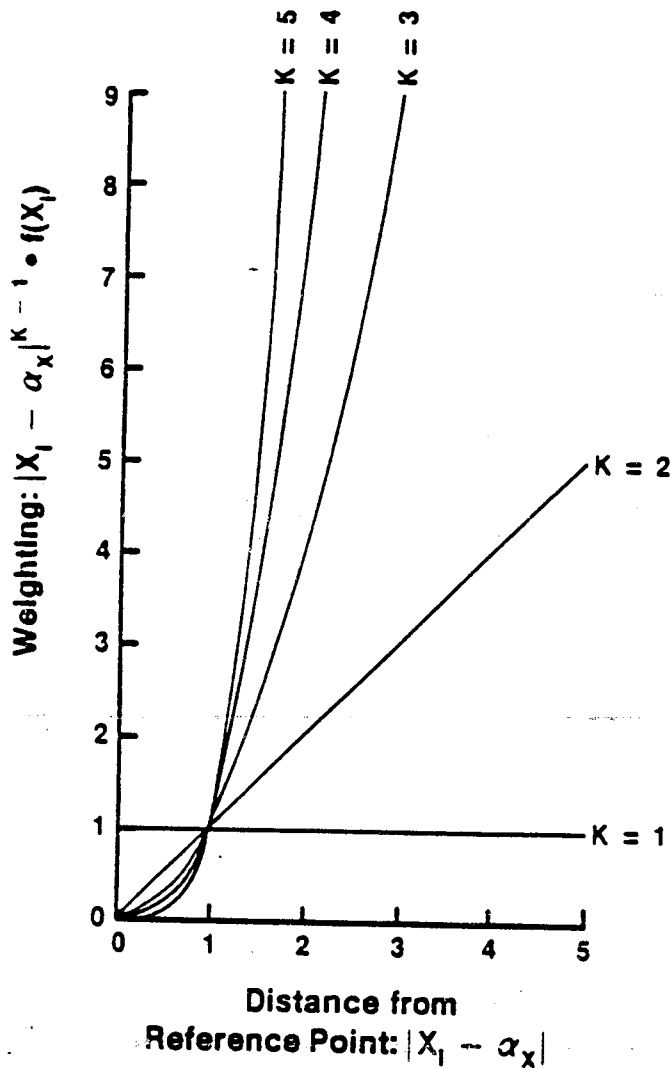


Figure 2. The weighting of the distance of the abscissa value x , from the reference point α_x , as a function of k , the order of the moment, and the distance $|x - \alpha_x|$ under the simplifying assumption that $f(x_i) = 1$.

asymmetry of the NB waveform—whereas the first n even moments provide the basis for an n -dimensional indicant of dispersion of the distribution of x , about α_x —that is, a vector-valued measure of dispersion of the NB waveform.

If, as in many instances in psychological research, one seeks to derive indicants with which to describe or compare the shape of NB waveforms, two transformations of Equation 2 are useful. The first, which we have already discussed, is to equate the waveforms with respect to the total amplitude by expressing each amplitude, $f(x_i)$, as a proportion of the total amplitude,

$$\frac{f(x_i)}{\sum_{i=1}^N f(x_i)}$$

The second is to take the $1/k$ th power of the k th moment, so that all the moments are expressed in the original units of measurement, such as centimeters, microvolts, microsiemens, or milliseconds. Note that taking the $1/k$ th power of the k th moment converts the even moments to true distance functions. Consider Equation 2 for k even. Clearly,

$$(\mu'_{k;x})^{1/k} = \left[\sum_{i=1}^N (x_i - \alpha_x)^k f(x_i) \right]^{1/k}$$

$$(\mu'_{k;x})^{1/k} = \left[\sum_{i=1}^N |x_i - \alpha_x|^k f(x_i) \right]^{1/k},$$

which is a Minkowski k -metric distance function (see Coombs, Dawes, & Tversky, 1970, pp. 60-62), and $f(x_i)$ weights $|x_i - \alpha_x|^k$. In mathematics, such distance functions are related to L_p norms. Thus, the transformed even moments, $(\mu'_{k;x})^{1/k}$, are true distance or dispersion measures in a mathematical sense. Moreover, if we substitute

$$\frac{f(x_i)}{\sum_{i=1}^N f(x_i)}$$

for $f(x_i)$ in the above argument, we see that the

$$\left[\frac{\mu'_{k;x}}{\sum_{i=1}^N f(x_i)} \right]^{1/k} = \gamma'_{k;x}$$

are also Minkowski distance functions and, therefore, dispersion measures as well. Finally, it should be noted that taking moments to the $1/k$ th power preserves all the information because the transformation is one to one.

In sum, we can define the moment-based probes of the topography of such a distribution as the bricks atop the beam in Figure 1 as

$$\gamma'_{k;x} = \left[\frac{\sum_{i=1}^N (x_i - \alpha_x)^k f(x_i)}{\sum_{i=1}^N f(x_i)} \right]^{1/k}, \quad k = 1, 2, \dots \quad (3)$$

The Reference Point

The fact that asymmetry and dispersion are always stated in terms of a reference point may not be obvious to some readers, nor may it be obvious that although we have treated α_x as an arbitrary reference point, the specification of the reference point is not arbitrary for the researcher because the reference point is fundamental to the interpretation of the indicants. This section is included, therefore, to illustrate the significance of reference points for the psychological investigator. Readers who are familiar with the moments and reference points may wish to proceed to the next section.

First Moment

In physics, the abscissa of the center of gravity is the point along a beam at which a fulcrum should be placed if the set of forces acting simultaneously on the beam is to produce no net rotation; that is, the first moment will be zero when the fulcrum is placed at the abscissa of the center of gravity. We can easily identify this point by solving for the reference point in Equation 3 given that $k = 1$ and $\gamma'_{1;x} = 0$. It is easy to see from inspecting Equation 3 that this is equivalent to solving for $\gamma'_{1;x}$ given that $k = 1$ and $\alpha_x = 0$, that is, the first moment about zero.

Waveform-dependent reference points. Suppose we adopt the first moment as our reference point when calculating the multi-dimensional indicants of asymmetry and of dispersion. Substituting this waveform-dependent reference point for α_x in Equation 3, we obtain

$$\gamma_{k;x} = \left[\frac{\sum_{i=1}^N (x_i - \mu_x)^k f(x_i)}{\sum_{i=1}^N f(x_i)} \right]^{1/k} \quad (4)$$

Because

$$E(X - \mu_x)^k = \sum_{i=1}^N (x_i - \mu_x)^k P(\{x_i\})$$

is the k th central moment of the distribution of bricks atop the beam and because

$$E^{1/k}(X - \mu_x)^k = \left[\sum_{i=1}^N (x_i - \mu_x)^k P(\{x_i\}) \right]^{1/k} \\ = \left[\frac{\sum_{i=1}^N (x_i - \mu_x)^k f(x_i)}{\sum_{i=1}^N f(x_i)} \right]^{1/k}$$

we see that the moment-based indicants defined by Equation 4 are simple one-to-one transformations of the central moments as defined in probability theory. The higher central moments, therefore, provide probes of the shape of the waveform with reference to the center of gravity.

Waveform-independent reference points. Now suppose we are interested in the shape of a waveform with reference to a fixed point common to all subjects and conditions. If we use the same reference point along the beam (call it x^*) for all waveforms of interest, then the weights associated with a specific x_i will be equal in the computation of a moment-based indicant if the amplitudes at x_i are equal. Thus, if we have two waveforms, f_1 and f_2 , $f_1(x_i) = f_2(x_i)$, then

$$|x_i - x^*|^{k-1} f_1(x_i) = |x_i - x^*|^{k-1} f_2(x_i).$$

If, on the other hand, we were to use the center of gravity, then the weights associated with a specific x_i would be unequal if the centers of gravity are unequal. Let μ_1 and μ_2 represent the centers of gravity for f_1 and f_2 , respectively, such that $f_1(x_i) = f_2(x_i) > 0$, $\mu_1 \neq \mu_2$. Clearly,

$$|x_i - \mu_1|^{k-1} f_1(x_i) \neq |x_i - \mu_2|^{k-1} f_2(x_i).$$

Thus, the weight associated with $|x_i - \mu_1|$ differs from the weight associated with $|x_i - \mu_2|$, even though the amplitudes at x_i are equal for the two waveforms. Therefore, if one wants to use indicants not only to distinguish among NB waveforms but also to contrast the underlying events as they unfold over a given (e.g., distance or time) domain, one may wish to select a reference point that is identical across conditions, that is, a waveform-independent reference point.

If, for instance, we have a beam of a fixed length, then the midpoint of the beam could serve as a fixed reference point. Beyond serving as a fixed reference point, the midpoint has a useful property. If there is an even number of observations x_i

($i = 1, 2, \dots, N$) and there are $N/2$ pairs of stacks (x_{j1}, x_{j2}) such that

$$x_{j1} < \text{midpoint} < x_{j2}$$

and

$$|x_{j1} - \text{midpoint}| = |x_{j2} - \text{midpoint}|$$

and if the stacks of a j th pair have identical amplitudes, then

$$|x_{j1} - \text{midpoint}|^{k-1} f(x_{j1}) = |x_{j2} - \text{midpoint}|^{k-1} f(x_{j2}).$$

In other words, the weights associated with x_{j1} and x_{j2} will be equal.

In the rare case in which the NB waveform is symmetrical about the midpoint, the weights associated with x_{j1} and x_{j2} will always be equal. The reason is that symmetry about the midpoint means that $f(x_{j1}) = f(x_{j2})$. If, on the other hand, the NB waveform is not symmetrical about the midpoint, then the weights associated with x_{j1} and x_{j2} will be unequal if $f(x_{j1}) \neq f(x_{j2})$. Thus, the higher order moment-based indicants in which the midpoint serves as the reference point weight distances with high amplitudes more than distances with low amplitudes even when the observations are equidistant from the midpoint.

Beginning and end of the beam. The preceding observations regarding the weighting of the x_i s apply generally, as illustrated in Figure 2. It should be noted, however, that when the beginning of the beam is the reference point (i.e., $\alpha_x = 0$), the odd moment-based indicants reduce to Minkowski k -metric distance functions (Coombs et al., 1970), so that all the moment-based indicants are measures of dispersion from the origin. Moreover, when the endpoint of the beam is the reference point, multiplication of the odd moments by -1 converts the odd moment-based indicants to Minkowski k -metric distance functions, so that the negatives of the odd moment-based indicants are measures of dispersion from the endpoint of the beam.

The most obvious choice for gauging the asymmetry of a distribution of bricks atop a beam is to choose a reference point within rather than at the extremes of the distribution. Two reasonable options are to (a) specify the first moment about the origin as the reference point to assess asymmetry about the center of gravity of the waveform and (b) designate the midpoint of the beam as the reference point to assess asymmetry within the distribution of bricks atop a given length beam. (When dealing with beams of differing lengths, these options remain the same, but distances can be expressed in standard measure prior to calculating the higher order moments for $k > 2$.)

To illustrate the fundamental difference between these two options, consider the waveforms depicted in Figure 3. The beam in each case is 7 units long, and the waveforms differ only in terms of where along the beam forces greater than zero were observed. It is clear from inspecting this figure and Equation 3 that if the reference point for each waveform is specified as the first moment about zero, then the asymmetry in these waveforms would be viewed as being equal and zero. If, however, the reference point is specified as being the midpoint of the beam, then the asymmetry in these waveforms would be different from zero, equal in absolute value, and opposite in sign.

In sum, any given reference point highlights particular features of a waveform. Therefore, choice of a reference point should be accompanied by a theoretical rationale for that choice. It is conceivable that there may be no literature or theory

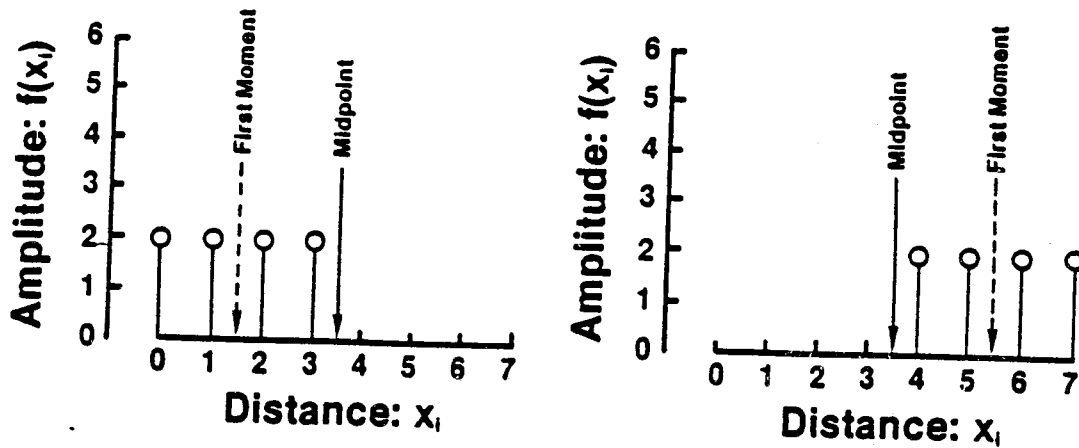


Figure 3. Two sample responses (or distributions of bricks) atop identical beams. The responses are viewed as being symmetrical if the center of gravity (i.e., the first moment about zero) is specified as the reference point when calculating the indicants of asymmetry and dispersion. Multidimensional indicants about the midpoint of the beam, however, indicate that the response on the left is asymmetrical with a preponderance of amplitudes (bricks) stacked on the lower end of the beam, whereas the response on the right is asymmetrical with a preponderance of amplitudes stacked at the upper end of the beam. Thus, it can be seen that although the use of either reference point produces an accurate, informative, and easily interpretable description of the responses, the ability of the investigator to specify what reference point to use offers greater flexibility and potential for describing or comparing responses in terms that are theoretically significant.

to guide the selection of a reference point in the early stages of research on a phenomenon. In these cases, one might conduct analyses in which the empirical utility of each of several reference points is examined.

The Time Domain

If the stacks of bricks are viewed as placed not at various positions across the beam but rather at a given position on the beam at various intervals in time, then an NB waveform can be defined by measuring the existing force at that position across time. This particular case in mechanics is analogous to a general case in psychological research in which a sequence of nonnegative amplitudes observed across time constitutes a response. Let t_i denote the time of the i th observation at some site, where t_i ranges from t_1, t_2, \dots, t_N , and let $f(t_i)$ denote the measure of the amplitude at time t_i ($f(t_i) \geq 0$). For purposes of illustration, each waveform depicted in Figure 4 is constructed to represent the amplitudes of a sequence of observations at some recording site across time. The amplitudes depicted in Figure 4 can represent a variety of measures in psychology, such as analog/digital conversions of physiological activity measured across several seconds.

If we simply extend the reasoning underlying the derivation of the indicants defined by Equation 4 to the time domain, we find that moment-based indicants of the form of the distribution of recorded amplitudes across time equated for the overall size of the response can be defined by

$$\gamma'_{k2} = \left[\frac{\sum_{i=1}^N (t_i - \alpha_i)^k f(t_i)}{\sum_{i=1}^N f(t_i)} \right]^{1/k} \quad (5)$$

where α_i now represents a reference point in time.

Illustrative Study

To illustrate the application of this topographical procedure, we selected for analysis four of the seven tasks used by Cacioppo et al. (1983). We recovered data from 6 subjects from the original study and added data from another 6 to this data set prior to analysis. The study involved subjects' squeezing a hand dynamometer in a prescribed fashion for 8-s epochs. The tasks selected for illustration here required that subjects (a) achieve and maintain a tension of 3 kg, (b) achieve and maintain a tension of 9 kg, (c) achieve a tension of 2 kg in 1 s and then increase the tension of the grip by 1 kg every second for the next 7 s, and (d) achieve a tension of 9 kg in 1 s and then decrease the tension by 1 kg every second for the next 7 s. Subjects practiced each task once and then performed each task six additional times; IEMG activity, sampled once approximately every 400 msec, was recorded over the superficial forearm flexors muscle region of the preferred hand. The order in which the tasks were performed was varied between subjects and served as a between-subjects replication factor in the analysis. (For details, see Cacioppo et al., 1983.)

Following analog-to-digital (A/D) data acquisition for each subject, the polygraph records of the raw EMG signals were inspected in order to allow the removal of artifacts. Next, the array of A/D observations from a subject that defined an IEMG response on a given trial was converted to an array of amplitudes expressed in microvolts, and the zero signal, expressed in microvolts, was subtracted from each entry in each array (Fridlund & Cacioppo, 1986). Indicants based on seven temporal moments and the first amplitude moment were calculated to summarize each IEMG response. Specifically, (a) the indicant based on the first moment about zero in the time domain was used to describe central tendency in the time domain; (b) a vector of indicants based on the second, fourth, and sixth moments about the mean in the time domain was calculated as a shape

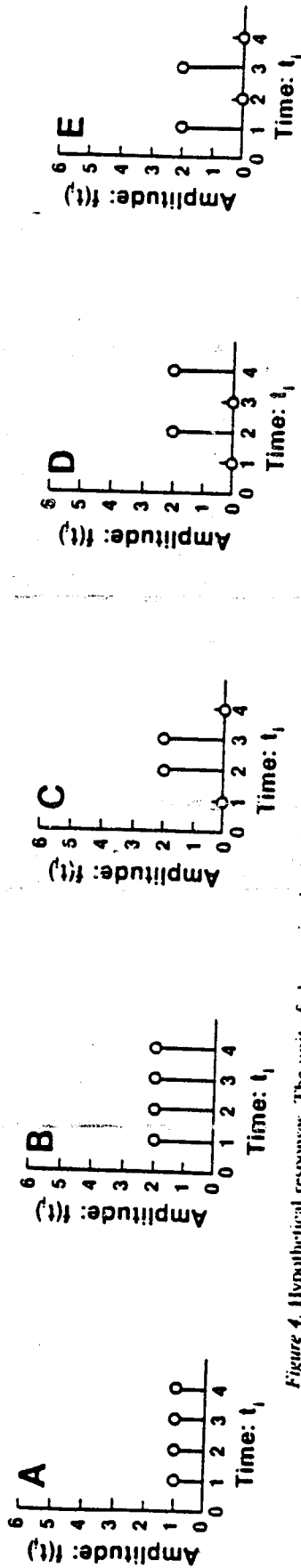


Figure 4. Hypothetical responses. The unit of observation in the time domain is depicted along the abscissa, and the amplitude of the response corresponding to each observation is presented along the ordinate.

descriptor regarding dispersion about the mean: (c) a vector of indicants based on the third, fifth, and seventh moments about the mean in the time domain was calculated to describe asymmetry about the mean; and (d) the indicant based on the first moment about zero in the amplitude domain (i.e., mean amplitude) was used to gauge the size of the response (an effective procedure because the number of observations was constant across responses).

To simplify the illustration, we averaged these indicants across the six repetitions of the tasks to increase the reliability and submitted them to a 2×7 (Replication \times Task) multivariate analysis of variance (MANOVA) using Wilks's criterion. Results of the MANOVA indicated that these indicants discriminated among the task-related responses: The main effect for task was significant, $F(12, 45) = 10.82, p < .001$. Neither any main effect for replication nor any Task \times Replication interaction approached significance, suggesting that the shapes of the distinctive task-induced IEMG responses were replicable.

We followed these analyses with Replication \times Task univariate analyses of variance (ANOVAs) to probe further what features of the task-related IEMG responses differed. Significant main effects for task were obtained for mean time, $F(3, 20) = 37.34, p < .001$; dispersion time, $F(3, 20) = 6.13, p < .01$; asymmetry time, $F(3, 20) = 25.68, p < .001$; and mean amplitude, $F(3, 20) = 17.49, p < .001$. Again, neither a main effect for replication nor any Task \times Replication interaction was significant in these ANOVAs, suggesting that specific features of the shape of the task-induced responses were also replicable.

The cell means and pairwise comparisons are summarized in Table 1. Inspection of the averaged task-related IEMG responses, which are summarized in Figure 5, confirms that the tasks were characterized by distinctive NB waveforms. More important, results of the MANOVA, ANOVAs, and pairwise comparisons illustrate that specific and replicable features of these responses that varied across tasks could be identified by using moment-based indicants. Thus, it can be seen that the moment-based indicants are not difficult to calculate or interpret and can provide a means of examining systematically whether and in what manner NB waveforms differ.

How Many Moments?

The number of moments necessary for characterizing the shape of an NB waveform increases as the complexity of the family of waveforms under consideration increases. For instance, if all members of a family are exponential distributions, then the first moment uniquely characterizes each member; if all members of a family are normal distributions, then the first two moments uniquely characterize each member; if all members of a family satisfy the Pearson system, then the first four moments suffice. (The Pearson system is a broad family of unimodal distributions; see Johnson & Kotz, 1970). If we have a family of discrete waveforms consisting of N points, then $N - 1$ moments fully characterize the normalized waveform; moreover, $N - 1$ moments and the total mass fully characterize the waveform (Norton & Arnold, 1985). If, on the other hand, the NB waveform is continuous, then all the moments are needed to fully characterize the waveform. The lower order moments provide the most information, with increments in information decreasing as each higher order moment is added. For instance,

Table 1
Mean Amplitude and Means of Time Indicators
as a Function of Task

Measure	Task			
	1	2	3	4
Mean amplitude	126.32 _a	257.98 _c	202.12 _b	130.95 _a
Mean time	4.46 _b	4.62 _b	5.08 _c	3.79 _a
Dispersion time	2.47 _a	2.37 _a	2.35 _a	2.42 _b
Asymmetry time	-0.60 _b	-0.70 _b	-2.02 _a	1.55 _c

Note. Means in a row with different subscripts differ significantly at $p < .05$ by the Duncan multiple-range test.

seven moments may prove capable of differentiating short, distinctive samples of IEMG responses even when the NB waveforms are multimodal. It might be added, however, that in conducting the analyses above, the moment-based indicators were extracted on a trial-by-trial basis; these descriptive parameters were averaged across trials within conditions in order to gain more reliable estimates of the treatment effects; and an internal replication of the study was conducted for determining the reliability and generalizability of the observations.

In the case of complex multimodal NB waveforms, the number of moments needed for an adequate characterization may be large. If one expresses the Fourier transform of the NB waveform in terms of the moments to be used and inverts the trans-

form, it is possible to evaluate the fidelity of the characterization (e.g., see Feller, 1966). To summarize, the investigator should be very cautious about using moment-based indicators to characterize complex multimodal NB waveforms in the absence of good evidence to support their use in such situations.

The Amplitude Domain

For any NB waveform in the time domain, there are p distinct amplitudes among the N amplitudes. Let us denote the j th distinct amplitude by f_j ($j = 1, 2, \dots, p$) and the frequency of occurrence of f_j by $g(f_j)$. Note that only in the extreme case in which there are N distinct $f(t_i)$ amplitudes in the distribution of times will $p = N$ and, necessarily, $g(f_j) = 1$. In all other cases (i.e., when there are fewer than N distinct $f(t_i)$ amplitudes), $0 < p < N$. In each case, an NB waveform in the time domain gives rise to one and only one frequency distribution of p distinct amplitudes.

An NB waveform in the amplitude domain gives rise to a unique distribution of times, however, only in the degenerative case in which $p = 1$, and therefore, $g(f_j) = N$ for one f_j . In all other cases, an amplitude distribution does not give rise to a unique NB waveform in the time domain because the amplitude distribution contains no information regarding the point in time (i.e., t_i) a given amplitude was observed. It is easy to see that by substituting equivalent terms, Equation 3 reduces to the following expression for the moment-based indicators in the amplitude domain:

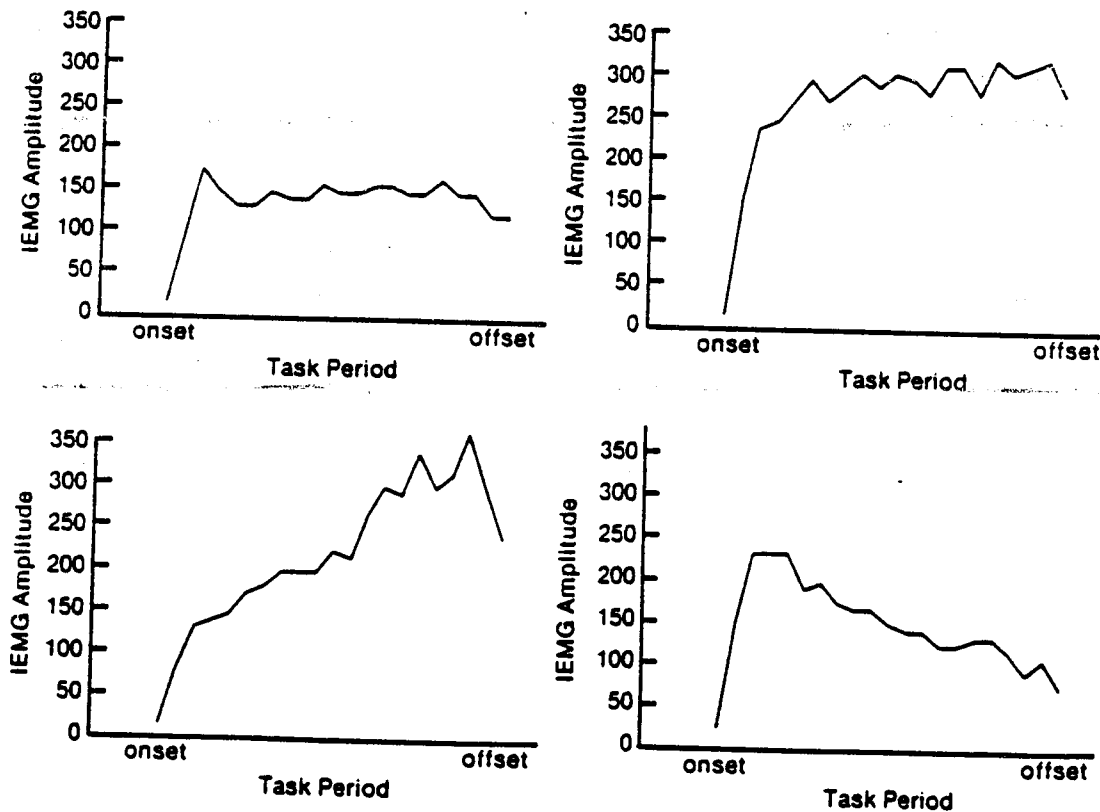


Figure 5. Averaged integrated electromyographic (IEMG) recordings obtained during tasks: (a) constant tension of 3 kg (upper left panel), (b) constant tension of 9 kg (upper right panel), (c) tension increasing from 2 to 9 kg (lower left panel), and (d) tension decreasing from 9 to 2 kg (lower right panel).

$$\gamma'_{k:f(t)} = \left[\frac{\sum_{i=1}^N (f(t_i) - \alpha_f)^k}{N} \right]^{1/k} \quad (6)$$

Interpretation of these shape descriptors is also a simple extension of our discussion above.

Illustrative Study

For purposes of illustration, the hypothetical responses shown in Figure 4 are expressed as distributions of amplitudes in Figure 6. Note that in Responses A and B, $p = 1$ and $g(f_j) = N$ for one j , whereas in Responses C, D, and E, $p = 2 < N$. Accordingly, it can be seen in this illustration that each NB waveform in the time domain gives rise to one and only one amplitude distribution, whereas an NB waveform in the amplitude domain gives rise to a unique distribution of times only when the response is uniform across time (e.g., $p = 1$). That is, unlike the indicants based on the moments of time, the indicants based on the moments of amplitude are insensitive to the manner in which the amplitudes are distributed over time. For instance, these indicants do not distinguish between high amplitudes constituting a response that are clustered together in time from equally high amplitudes that are distributed across the recording interval in what appears as shorter bursts of activity (e.g., see Responses C-E in Figures 4 and 6). These observations underscore the fact that the indicants based on moments in the time and amplitude domains can provide complementing characterizations of NB waveforms.

To illustrate simply how one might probe NB waveforms by using indicants based on the higher order amplitude moments, we calculated six additional indicants based on amplitude moments to characterize each IEMG response obtained in the empirical study described above. Specifically, (a) indicants based on the second, fourth, and sixth moments about mean amplitude were calculated to gauge dispersion, and (b) indicants based on the third, fifth, and seventh moments about mean amplitude were calculated to gauge asymmetry. Results of 2×7 (Replication \times Task) ANOVAs revealed significant task main effects for dispersion amplitude, $F(3, 20) = 13.31, p < .001$, and asymmetry amplitude, $F(3, 20) = 11.43, p < .001$. Cell means and pairwise comparisons are summarized in Table 2. It can be seen that the amplitude moments can be quite informative. For instance, although mean amplitudes for Tasks 1 and 4 were approximately equal (see Table 1), the more homogeneous set of amplitudes obtained in Task 1 became evident in the measure of dispersion amplitude (see Table 2).

Summarizing thus far, the amplitude moments may be of interest in the study of psychological responses for three major reasons: (a) Mean amplitude, which is a common measure in psychophysiological research for summarizing responses of the form depicted in Figure 4, is the first moment about the origin of the distribution of amplitudes of an NB waveform (see Figure 6), and the first moment about the origin in the amplitude domain can be used in conjunction with the number of observations (N) to gauge the size of the response (i.e., the total mass of the discrete NB waveform). (b) Multidimensional indicants based on the higher order moments (i.e., $k > 1$) in the amplitude domain can be used to gauge the asymmetry and dispersion of the distribution of amplitudes. (c) Multidimensional indicants

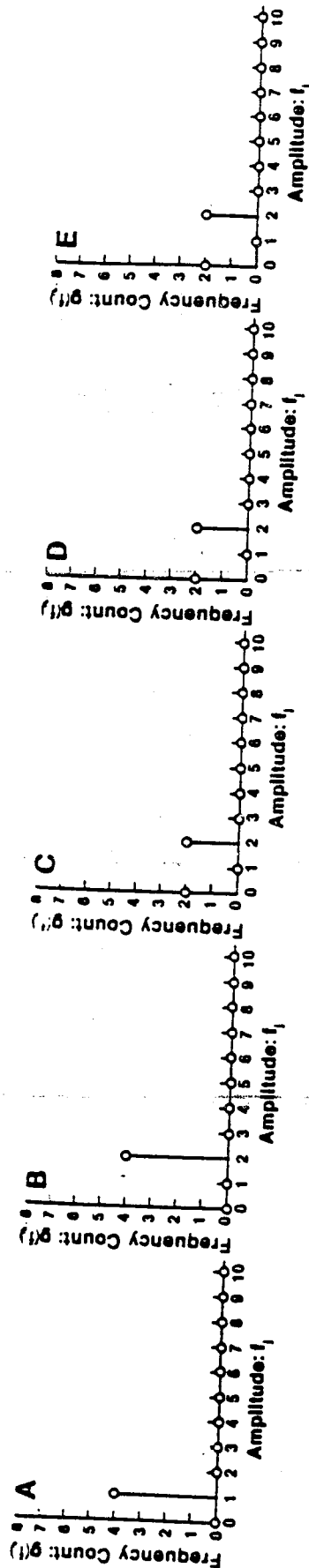


Figure 6 The responses from Figure 4 expressed as distributions of amplitudes.

Table 2
Means of Higher Order Amplitude Indicators
as a Function of Task

Measure	Task			
	1	2	3	4
Dispersion amplitude	83.53 _b	146.76 _c	157.77 _c	108.08 _b
Asymmetry amplitude	-45.38 _b	-60.77 _a	103.53 _c	84.21 _b

Note. Means in a row with different subscripts differ significantly at $p < .05$ by the Duncan multiple-range test.

based on amplitude moments can be used to partially characterize arbitrary bounded waveforms. We next turn to the importance of this point.

Amplitude Moments for Arbitrary Bounded Waveforms

A number of important measures of psychophysiological activity in the time domain have amplitudes that are bounded in all cases of practical interest but assume negative as well as non-negative values. We call such waveforms *arbitrary bounded waveforms*. Because the amplitudes can assume negative values, it is clear that such waveforms are not NB waveforms. Specifically, such waveforms cannot be represented as density functions in the time domain, and therefore, a moment-based analysis is inappropriate. If, on the other hand, we consider the histograms of amplitudes, then a moment-based analysis is appropriate, and the procedures outlined in this article are straightforward extensions of the classical distribution descriptors that have recently been used in EMG (e.g., Cacioppo et al., 1983) and EEG research (e.g., Bronzino et al., 1981). In fact, in all cases of practical interest, the distribution of amplitudes is an NB waveform and, therefore, amenable to characterization by the moment-based indicators.

The importance of amplitude measures in quantifying such psychophysiological responses as the EMG, EEG, and event-related potential has long been recognized. For instance, mean and peak amplitudes are perhaps the most widely used measures of the EMG in psychophysiology (see Goldstein, 1972; Lippold, 1967; McGuigan, 1978). Quantification of amplitudes has also been important in the study of EEG. In fact, Hans Berger (1929/1976), who published the first report on the EEG in humans, suggested that quantifications be performed on both frequencies and amplitudes.

Moreover, in their authoritative text on EEG technology, Cooper, Osselson, and Shaw (1980) noted, "One of the obvious features of an EEG is the amplitude of the fluctuations" (p. 235). They went on to mention four principal measures of amplitude: (a) the average peak-to-peak amplitude, (b) the envelope of the waveform, (c) the average absolute deviation of the amplitudes from zero baseline, and (d) the square root of the average squared deviation of the amplitudes from zero baseline (the root-mean-square from zero baseline). If the mean amplitude is zero, the fourth one above is the standard deviation of the amplitudes. Thus, it is a moment-based indicant with $k = 2$ and the reference point at zero (see Equation 6). Cooper et al. (1980) also mentioned the importance of considering the entire distribution of amplitudes:

One way of gaining an insight into the characteristics of the amplitude fluctuations of EEG signals is to use a measure known as the amplitude probability density function. This is a graph showing the probability of occurrence of a particular amplitude value. It has an amplitude scale for the x-axis and a probability scale for the y-axis. (p. 236)

The amplitude distribution is often found to be normally distributed (Cooper et al., 1980; Saunders, 1963, 1972). This is especially true when subjects are idle (Elul, 1967, 1969). During performance of mental arithmetic, however, Elul (1967, 1969) found, the amplitude distribution was less likely to fit a normal distribution than when subjects were idle. Elul's (1969) approach involved classifying the observed amplitude distributions as Gaussian (normal) or non-Gaussian (nonnormal) on the basis of chi-square tests of goodness of fit with mean and standard deviation estimated from the data.

Elul (1967) presented an interesting theory to explain the transformation of the amplitude distribution from normal in an idle state to nonnormal in a mentally active state. He suggested that the gross EEG is the sum of the outputs of a large number of mutually independent generators. Under broad conditions, the central limit theorem implies that the sum of the outputs of those mutually independent generators will be approximately normally distributed. If, however, the subject is mentally active, Elul (1967) suggested, the generators become mutually interdependent. Therefore, the central limit theorem no longer applies, so the sum of the outputs of the component generators is transformed to a non-Gaussian distribution.

A similar phenomenon can be demonstrated in the area of mental testing. Suppose that a total test score (Y) is the sum of a large number of component test-item scores (X_i , $i = 1, 2, \dots, N$), so that

$$Y = \sum_{i=1}^N X_i.$$

Suppose further that all component test-item scores are correlated with some common underlying factor and are mutually independent if that correlation is zero. Lord (1952) showed that one can systematically modify the shape of the distribution of test scores by manipulating the correlation of the component test-item scores with the common underlying factor. Figure 7 (reprinted from Lord's, 1952, Figure 4, p. 38) shows four frequency distributions generated by manipulating that correlation. It is apparent that as the correlation increases, the moment-based indicators of dispersion tend to increase.

Whereas Elul's (1967, 1969) theory of amplitude distributions is very interesting, it should be clear from the example displayed in Figure 7 that Elul's (1967, 1969) method of assessing amplitude distributions has weaknesses. For one thing, his dichotomous classification scheme does not distinguish among Gaussian distributions. Gaussian distributions may differ in both mean and standard deviation. For another—perhaps the more important—his classification scheme throws all non-Gaussian distributions together. Non-Gaussian distributions may differ in a variety of ways, and Elul's (1967, 1969) dichotomous classification disregards that variety.

The moment-based indicators for characterizing an NB waveform in the amplitude domain, on the other hand, offer a systematic and comprehensive alternative for analyzing amplitude

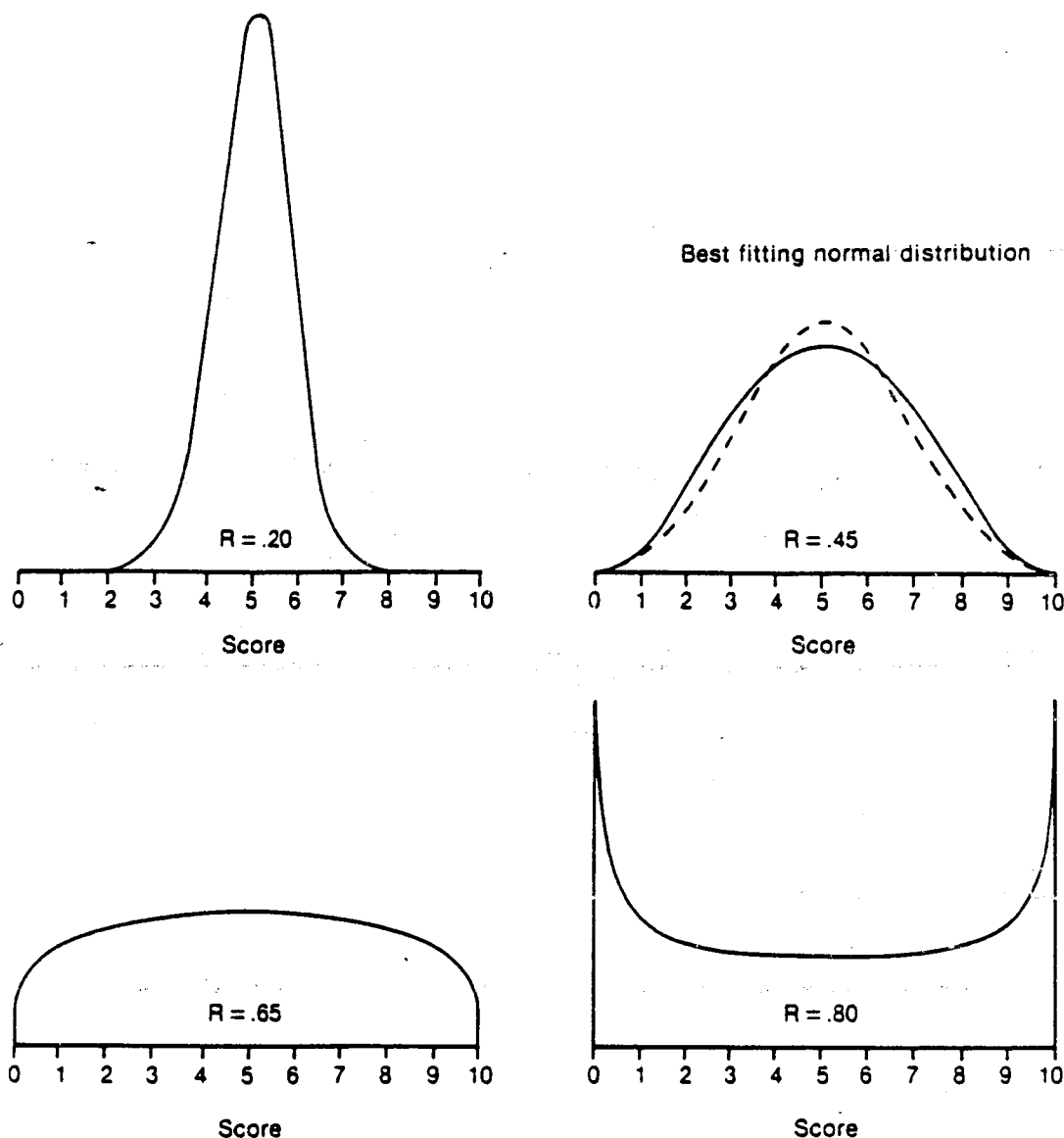


Figure 7. Frequency distributions of test scores as a function of the correlation (R) between a common underlying trait and the item scores. (From "A Theory of Test Scores" by F. Lord, 1952, *Psychometric Monographs*, Whole No. 7, p. 38. Copyright 1952 by F. Lord. Reprinted by permission.)

distributions. If all amplitude distributions are Gaussian, then the arithmetic mean (first moment about the origin) and the standard deviation (a moment-based indicant about the mean with $k = 2$) fully characterize those distributions. If, however, the distributions are not all Gaussian, then the probes need not stop at $k = 2$ (as occurs when the root-mean-square or standard deviation is used to characterize the amplitude distribution), and the moment-based indicants provide a superior means of characterizing the waveform through multidimensional indicants of asymmetry and dispersion about a reference point. Bronzino et al.'s (1981) adoption of skewness and kurtosis to quantify the EEG in the amplitude domain, therefore, represented a significant advance over Elul's (1967, 1969) method, even though these classical descriptive parameters represent a special and more limited case of the multidimensional indicants

outlined here. Moreover, the moment-based indicants do not require such simplifying assumptions as the Gaussian assumption or that the mean is always zero. In addition, the indicants outlined here provide greater flexibility by retaining comparable units of measurement as k varies and by allowing the investigator to select the reference point or points of greatest theoretical or empirical interest.

Summing up, quantification of amplitude distributions through moment-based indicants is of demonstrated value when dealing with waveforms whose amplitudes can take on negative as well as nonnegative values and whose amplitude distributions are not necessarily Gaussian. This approach also offers the advantage of providing reduction of data and readily permitting intra-individual or interindividual comparisons.

The Frequency Domain

Thus far, we have focused on the characterization of waveforms in the time and amplitude domains. There are, however, a variety of waveforms in psychophysiology that are usefully represented in the frequency domain, for example, the EEG (e.g., see Cogter, Dymond, & Serafetinides, 1979; Cooper et al., 1980).

One begins with a collection of amplitudes observed sequentially in time. To obtain a frequency representation of that collection of observations, one performs a spectral analysis: that is, one computes the power spectrum or spectral density function of that collection of observations. The actual computation is often done with an algorithm known as the *fast Fourier transform* (FFT), an efficient method for computing a discrete approximation to the Fourier transform. If there are a few frequencies at which the power is almost totally concentrated, then we can characterize the power spectrum in terms of those few frequencies. If, on the other hand, the power spectrum is smeared over a broad spectral band in a rather smooth fashion, then the power spectrum cannot be fully characterized by a few frequencies. In that case, it may be useful to characterize the power spectrum in terms of the moment-based indicants described earlier.

Assume that the power spectrum is band limited so that the power spectrum is an NB waveform. In fact, most measuring instruments are band limited in that they do not respond to frequencies above a certain maximum (Chatfield, 1980). The power spectrum is sometimes called the *power density spectrum* (Cooper et al., 1980), the *spectral density function* (Chatfield, 1980), or the *power spectral density* (Saltzberg & Burch, 1971). Those terms make good sense because the power spectrum is a density function although not necessarily standardized to a unit mass. In fact, if we divide the power at each frequency by the total power, the power spectrum is thereby transformed to a probability density function. Hence, the moment-based indicants can be computed in the frequency domain without special attention or restrictive assumptions (Cacioppo & Dorfman, 1984). In accord with the points made earlier with regard to the time and amplitude domains, the moments of frequency uniquely and fully characterize the power spectrum. In short, the topography of the power spectrum may provide valuable information beyond that of allowing for easy identification of hidden periodicities concentrated in a few frequencies (e.g., see Granger, 1966, for a discussion of a typical shape of a power spectrum observed in economics).

It is also of some interest that EEG scientists have suggested that indicants based on the moments may provide a useful summary of the power spectrum, or equivalently, the power spectral density (Hjorth, 1970, 1973, 1975; Saltzberg & Burch, 1971; Saltzberg et al., 1985). As noted, Hjorth (1970) suggested that the EEG be summarized by the parameters of activity, mobility, and complexity. The first parameter, activity, is the total mass of the two-sided power spectrum or, equivalently, the second moment of the amplitudes taken from zero baseline, often called *mean power* (Hjorth, 1970, 1975). The second parameter, mobility, is the standard deviation of the two-sided power spectrum normalized to an area of one (Hjorth, 1975). Note that the two-sided power spectrum is symmetrical about zero frequency, with identical branches stretching into both negative

and positive frequencies with mean frequency equal to zero (Hjorth, 1970). Hence, Hjorth (1970) did not measure skewness or asymmetry because all odd moments are zero, and therefore, skewness is always zero. The third parameter, complexity, can be shown to equal the square root of a common measure of kurtosis (β_2) if we convert the two-sided power spectrum to a mass of one. Specifically,

$$\text{Complexity} = (\beta_2)^{1/2} = \left[E \left(\frac{X - \mu}{\sigma} \right)^4 \right]^{1/2},$$

where $\mu = 0$ for the two-sided power spectrum. Also notice that it is the square root of the fourth moment of the power spectrum transformed to a probability density function with a variance of one. As discussed earlier, Hjorth's (1970, 1973, 1975) complexity is, therefore, a measure of the dispersion of order four of the unit-mass power spectrum.

Hjorth's (1970, 1973, 1975) descriptors have been found to be quite useful. For instance, Figure 8 illustrates their use in distinguishing between different states of sleep, including deep sleep and paradoxical sleep (rapid eye movement; Hjorth, 1973). Hjorth's (1970, 1973, 1975) three descriptors can also be used to distinguish between resting state with eyes open versus eyes closed and EEG reactions to performance on arithmetic or vocabulary tests (Chavance & Samson-Dollfus, 1978); they can be used to assess the effects of hemodialysis on, for example, visual discrimination, memory, and tapping speed (Spehr et al., 1977); and they can be used to provide a topographical display of localized EEG abnormalities (Persson & Hjorth, 1983). Thus, Hjorth's (1970, 1973, 1975) approach suggests that the moment-based representation of the power spectrum outlined in this article may be of value. Whereas the weakness of Hjorth's (1970, 1973, 1975) three descriptors lies in the fact that they do not fully characterize the power spectrum (e.g., see Denoth, 1975), the moment-based indicants do more fully characterize the power spectrum. No simple relation appears to exist between the moments of the power spectrum and the moments of the amplitude density function. There is, on the other hand, a straightforward relation between the moments of the power spectrum and the derivatives of the waveform in the time domain. Specifically, the second moment of the n th-order derivative of the waveform in the time domain equals the $2n$ th even moment of the two-sided power spectrum (Denoth, 1975).

As another illustration of the utility of moment-based indicants, let us look at a representation of the physically realistic one-sided power spectrum by the moment-based indicants. In particular, let us look at some one-sided power spectra reported in an interesting study of the genetic determination of EEG spectra by Lykken, Tellegen, and Thorkeison (1974). They obtained power spectra from EEG samples through the FFT algorithm. The power spectrum was converted to a magnitude spectrum by taking the positive square root of power, and then the total mass of the spectrum was standardized to unity. Figure 9 contains some illustrative magnitude spectra taken from monozygotic and dizygotic twins at rest. It is quite clear from a visual inspection of Figure 9 that the monozygotic twins are much more alike than the dizygotic twins in the magnitude spectra. This, in fact, was Lykken et al.'s solidly based conclusion. But, most important for our illustration, moment-based indicants

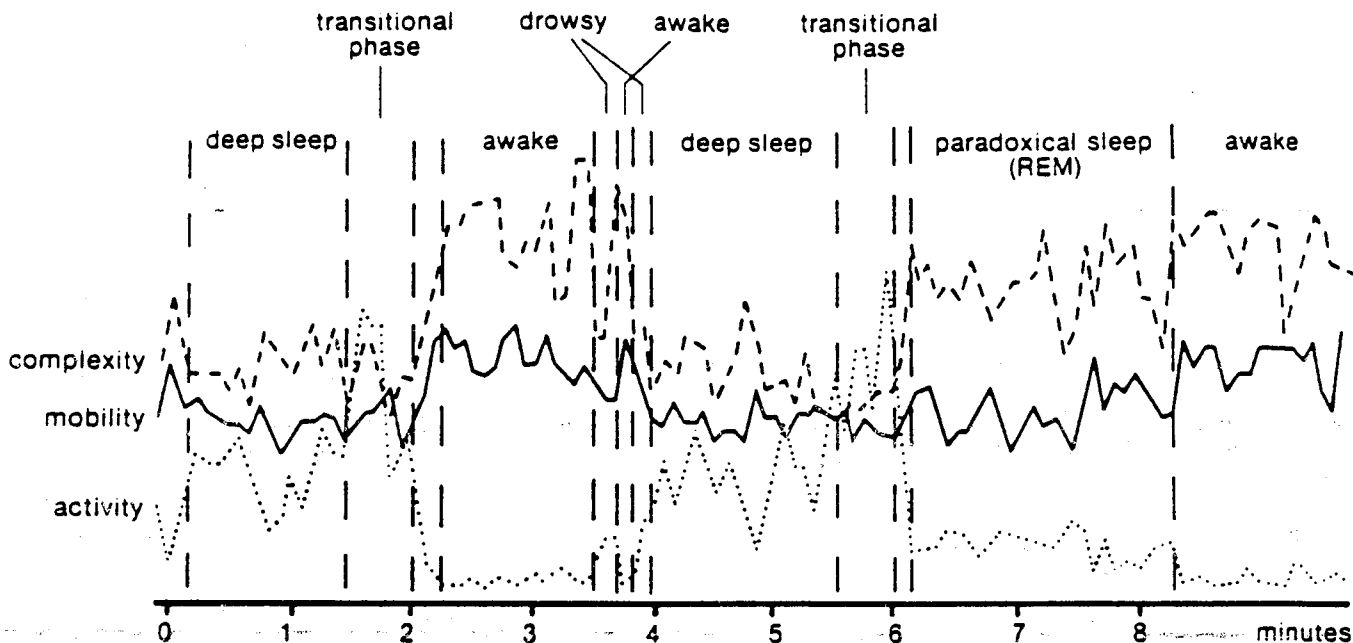


Figure 8. Hjorth's (1973) descriptors of activity, mobility, and complexity computed for every epoch of 5 s during a fronto-parietal recording from a rat. The descriptors illustrate characteristic patterns corresponding to distinct states of sleep and waking. (From "The Physical Significance of Time Domain Descriptors in EEG Analysis" by B. Hjorth, 1973, *Electroencephalography and Clinical Neurophysiology*, 34, p. 322. Copyright 1973 by B. Hjorth. Reprinted by permission.)

offer a rigorous means of comparing and contrasting these EEG power spectra on center of gravity (mean frequency), dispersion, and asymmetry. Note that because the bandwidth of a power spectrum is essentially a measure of the spread of the spectrum, it is worth mentioning that the moment-based indicants of dispersion provide a multidimensional measure of the bandwidth of the spectrum.

The results of a moment-based quantification of the magnitude spectra are shown in Table 3. The magnitude spectra depicted in Figure 9 were expressed as eight separate distributions of frequencies, and moment-based indicants were calculated for each. No statistical tests were performed, because of the illustrative nature of this example, but perusal of the moment-based indicants in Table 3 shows that quantifiable differences in the center of gravity (mean frequency), dispersion, and asymmetry exist within pairs of twins, particularly dizygotic pairs.

To gauge how dissimilar each twin-spectra pair was, we formed moment-based indexes of dissimilarity in mean frequency, in dispersion about mean frequency, and in asymmetry about mean frequency. Let $\gamma_{2k}^{(m)}$ denote the moment-based indicant of order k taken about the reference point α for twin m ($m = 1, 2$). Thus, $\gamma_{1,0}$ is the arithmetic mean. The index of dissimilarity in mean (center of gravity) was defined as

$$|\gamma_{1,0}^{(1)} - \gamma_{1,0}^{(2)}|;$$

the index of dissimilarity in dispersion was defined as

$$\sum_{k=1}^n |\gamma_{2k,\gamma_1}^{(1)} - \gamma_{2k,\gamma_1}^{(2)}|,$$

where $\gamma_1 = \gamma_{1,0}$; and the index of dissimilarity in asymmetry was defined as

$$\sum_{k=2}^n |\gamma_{2k-1,\gamma_1}^{(1)} - \gamma_{2k-1,\gamma_1}^{(2)}|.$$

Briefly, as n gets large, the moments capture more fully all the information in an NB waveform, and therefore, the dissimilarity indexes provide increasingly satisfactory measures of the distance separating two NB waveforms.

The interesting task, of course, is to identify precisely the manner in which these waveforms differ. Therefore, the dissimilarity indexes defined above for center of gravity, dispersion, and asymmetry were calculated to gauge how similar or dissimilar those specific features of the paired waveforms were. Recall that those three features fully characterize the waveform when those features are defined in terms of multidimensional moment-based indicants. Results, summarized in Table 3, reveal that the EEG spectra of monozygotic twins were more similar than the EEG spectra of dizygotic twins in center of gravity (mean frequency), dispersion about mean frequency, and asymmetry about mean frequency. Inspection of the moment-based indicants provides yet more information about these EEG spectra. We can see, for instance, that the preponderance of EEG activity in these spectra was less than 10 Hz, with mean frequency ranging from 8.43 to 9.93 Hz. In addition, the moment-based indicants of dispersion were greater for power spectra that appear smeared as opposed to peaked, in accordance with what we would expect of measures of dispersion. In conclusion, the moment-based indicants may provide a useful summary of the

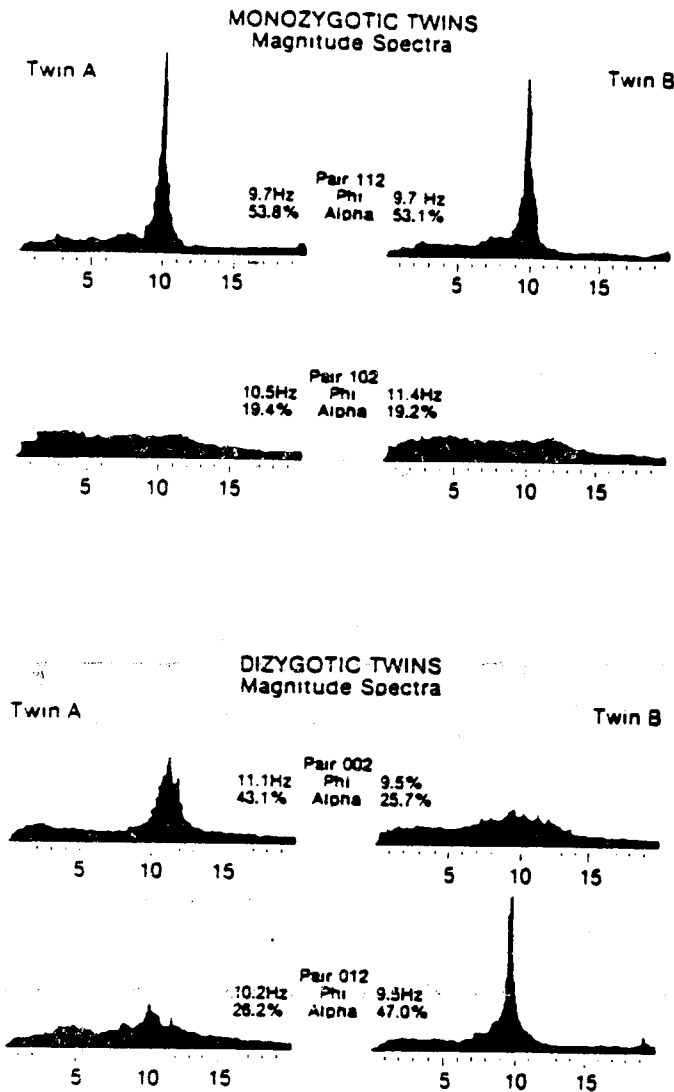


Figure 9. Electroencephalogram magnitude spectra (the positive square root of the power spectra) of monozygotic and dizygotic twins at rest. The magnitude spectra were standardized to a mass of one. Phi in the figure is the median frequency within the "alpha bump," and alpha is the proportion of the total spectrum contained within a 3-Hz band centered on phi. From "Genetic Determination of EEG Frequency Spectra" by D. T. Lykken, A. Tellegen, & K. Thorkelson, 1974, *Biological Psychology*, 1, pp. 252, 254. Copyright 1974 by D. T. Lykken, A. Tellegen, & K. Thorkelson. Adapted by permission.)

physically realistic one-sided power spectrum as well as the two-sided power spectrum.

Efficient Procedures for Estimating Moments in the Frequency Domain

Zero crossings and the spectral moments. If we normalize the two-sided power spectrum to a total mass of one, there is a simple relation to zero crossings per second of the signal in the time domain and the moments about zero of the normalized two-sided power spectrum. Specifically, for the band-limited case $|\omega| \leq F$,

$$\begin{aligned} \left(\frac{N_1}{2}\right)^2 &= \frac{\int_{-F}^F \omega^{2n} P(\omega) d\omega}{\int_{-F}^F P(\omega) d\omega} \\ &= 2 \int_0^F \omega^{2n} P(\omega) d\omega / 2 \int_0^F P(\omega) d\omega \\ &= \int_0^F \omega^{2n} P(\omega) d\omega / \int_0^F P(\omega) d\omega, \end{aligned}$$

where the left-hand side of the equation is the square of the number of zero crossings per second of the $(n-1)$ th derivative of the time-domain signal and the right-hand side is the $2n$ th even moment of the normalized two-sided power spectrum (Saltzberg & Burch, 1971; Saltzberg et al., 1985). For instance, $(N_1/2)^2$, where N_1 is the number of zero crossings per second of the signal, is the second spectral moment; $(N_2/2)^2$, where N_2 is the number of zero crossings per second of the derivative of the signal, is the fourth spectral moment. This important result permits one to obtain the even moments of the two-sided power spectrum by counting zero crossings (Saltzberg, 1973; Saltzberg & Burch, 1971). The method is economical but somewhat less robust than a new method of computing spectral moments from the autocorrelation function (Saltzberg et al., 1985).

The autocorrelation function and the spectral moments. Saltzberg et al. (1985) recently developed an innovative procedure for computing the moments of the two-sided or the physically realistic one-sided power spectrum. The procedure involves the summation of a small number of weighted samples of the autocorrelation function. The method is easy to apply, is economical of time and effort, and is an accurate approximation. Moreover, it is robust with respect to the underlying stochastic process. The method is of particular value in the on-line monitoring of EEG over long periods of time. Saltzberg et al. suggested that the shape of the normalized power spectrum be summarized on-line by the four standard moment-based parameters of mean, variance, skewness, and kurtosis. With regard to the utility of those moments-based parameters, they concluded the following:

Of major significance in clinical applications, these parameters provide easily interpretable measures of change in basic stochastic properties of complex time series and therefore offer an efficient and mathematically rigorous approach to the analysis and monitoring of complex biological signals such as the EEG. (Saltzberg et al., 1985, p. 93)

In sum, Saltzberg et al. outlined an efficient procedure for estimating moments in the frequency domain, and they found those shape descriptors to be theoretically and empirically useful.

Estimation of Confidence Intervals and Hypothesis Testing

Replications provide the basis for estimation of confidence intervals and hypothesis testing for moment-based indicants. Replications within subjects should provide for estimation of within-subject variability, and replications between subjects should provide for estimation of between-subjects variability (e.g., see Cacioppo et al., 1983). Under the assumption of robustness, estimating and testing based on classical univariate

Table 3
Moment-Based Indicators of Magnitude Spectra

Indicant	Monozygotic twins				Dizygotic twins			
	Pair 112		Pair 102		Pair 002		Pair 012	
	A	B	A	B	A	B	A	B
Mean frequency								
Dissimilarity ^a	0.01		0.03		0.87		0.15	
$\gamma_{1.0}$	9.48	9.47	8.43	8.46	9.93	9.06	9.50	9.65
Dispersion (bandwidth) about mean frequency								
Dissimilarity ^b	0.14		0.06		0.75		1.47	
$\gamma_{2.71}$	3.66	3.59	4.81	4.85	4.27	4.59	4.53	3.68
$\gamma_{4.71}$	5.34	5.29	5.98	5.97	5.58	5.78	5.68	5.29
$\gamma_{6.71}$	6.34	6.32	6.84	6.83	6.35	6.58	6.43	6.20
Asymmetry about mean frequency								
Dissimilarity ^a	0.26		0.10		16.32		0.53	
$\gamma_{3.71}$	2.82	2.96	3.45	3.40	-2.73	2.60	2.75	2.57
$\gamma_{5.71}$	5.12	5.19	5.76	5.73	-3.66	5.06	4.93	4.74
$\gamma_{7.71}$	6.35	6.40	6.97	6.95	4.11	6.38	6.12	5.96

^a Dissimilarity indexes calculated by using moment-based indicants about the origin (0). ^b Dissimilarity indexes calculated by using moment-based indicants about the mean.

and multivariate normal distribution theory should be appropriate. On the other hand, there are methods for interval estimation and hypothesis testing that are distribution-free—that is, they are not based on classical Gaussian distribution theory—and yet are very powerful. One such technique, the jackknife technique, can be applied without difficulty to the present class of statistics if one wishes to avoid classical Gaussian distribution theory (Arvesen & Salsburg, 1975; Efron, 1982; Rey, 1978; Tukey, 1969). As an added attraction, the jackknife technique reduces statistical bias (Rey, 1978). Two very readable introductions to the jackknife technique—written for psychologists—can be found in Mosteller and Tukey's (1968) chapter and in Tukey's (1969) article. In short, powerful methods for interval estimation and hypothesis testing are provided by classical univariate and multivariate statistics given Gaussian assumptions and by distribution-free procedures if one wishes to avoid assumptions about the data distribution.

Concluding Remarks

In sum, if, as Fisher (1922) suggested, one major purpose of statistics is to summarize as much as possible the useful information contained in a data set, then we believe that the computation of the moments appears to have a good chance of accomplishing this goal for NB waveforms in the time domain and for arbitrary bounded waveforms in the amplitude and frequency domains. This approach not only offers the advantage of providing reduction of data but also readily permits intra-individual comparisons. Two NB waveforms are identical if and only if all their moments and their total mass are equal. Finally, although a waveform moment analysis may shed light on aspects of responses that are not readily captured by other representations, the moment-based representation of a waveform should not be considered solely as a rival to other repre-

sentations; each representation contributes something to our understanding of the underlying process in question (Box & Jenkins, 1970, p. 44).

References

- Arvesen, J. N., & Salsburg, D. S. (1975). Approximate tests and confidence intervals using the jackknife. In R. M. Elashoff (Ed.), *Perspectives in biometrics* (Vol. 1, pp. 123-147). New York: Academic Press.
- Berger, H. (1976). On the electroencephalogram in man. In S. W. Porges & M. G. H. Coles (Eds.), *Psychophysiology* (pp. 9-14). Stroudsburg, PA: Dowden, Hutchinson, & Ross. (Original work published 1929)
- Box, G. E. P., & Jenkins, G. M. (1970). *Time series analysis: Forecasting and control*. San Francisco: Holden-Day.
- Bracewell, R. N. (1978). *The Fourier transform and its applications* (2nd ed.). New York: McGraw-Hill.
- Bronzino, J. D., Kelly, M. L., Cordova, C. T., Oley, N. H., & Morgane, P. J. (1981). Utilization of amplitude histograms to quantify the EEG effects of systemic administration of morphine in the chronically implanted rat. *IEEE Transactions on Biomedical Engineering*, *BME-28*, 673-678.
- Cacioppo, J. T., & Dorfman, D. D. (1984). Moments in psychophysiological research: Topographical analysis of non-negative bounded waveforms. *Psychophysiology*, *21*, 571.
- Cacioppo, J. T., Marshall-Goodell, B., & Dorfman, D. D. (1983). Skeletomuscular patterning: Topographical analysis of the integrated electromyogram. *Psychophysiology*, *20*, 269-283.
- Cacioppo, J. T., Petty, R. E., & Marshall-Goodell, B. (1984). Electromyographic specificity during simple physical and attitudinal tasks: Location and topographical features of integrated EMG responses. *Biological Psychology*, *18*, 85-121.
- Cacioppo, J. T., Petty, R. E., & Morris, K. J. (1985). Semantic, evaluative, and self-referent processing: Memory, cognitive effort, and somatovisceral activity. *Psychophysiology*, *22*, 371-384.
- Chatfield, C. (1980). *The analysis of time series: An introduction* (2nd ed.). New York: Chapman and Hall.
- Chavance, M., & Samson-Dollfus, D. (1978). Analyse spectrale de

- l'EEG de l'enfant normal entre 6 et 16 ans: Choix et validation des paramètres les plus informatif [EEG spectral analysis of the normal child from 6 to 16 years]. *Electroencephalography and Clinical Neurophysiology*, 45, 767-776.
- Chissom, B. S. (1970). Interpretation of the kurtosis statistic. *The American Statistician*, 24(4), 19-22.
- Coger, R. W., Dymond, A. M., & Serafetinides, E. A. (1979). Methods of electrophysiological research. In E. A. Serafetinides (Ed.), *Methods of biobehavioral research* (pp. 111-122). New York: Grune & Stratton.
- Coombs, C. H., Dawes, R. M., & Tversky, A. (1970). *Mathematical psychology: An elementary introduction*. Englewood Cliffs, NJ: Prentice-Hall.
- Cooper, R., Osselson, J. W., & Shaw, J. C. (1980). *EEG technology* (3rd ed.). London: Butterworths.
- Darlington, R. B. (1970). Is kurtosis really "peakedness"? *The American Statistician*, 24(2), 19-22.
- Denoth, F. (1975). Some general remarks on Hjorth's parameters used in EEG analysis. In G. Dolce & H. Kunkel (Eds.), *CEAN: Computerized EEG analysis* (pp. 9-18). Stuttgart, FRG: Gustav Fischer Verlag.
- Efron, B. (1982). *The jackknife, the bootstrap, and other resampling plans*. Philadelphia, PA: Society for Industrial and Applied Mathematics.
- Elul, R. (1967). Statistical mechanisms in generation of the EEG. In L. J. Fogel & F. W. George (Eds.), *Progress in biomedical engineering* (pp. 131-150). Washington, DC: Spartan Books.
- Elul, R. (1969). Gaussian behavior of the electroencephalogram: Changes during performance of mental task. *Science*, 164, 328-331.
- Feller, W. (1966). *An introduction to probability theory and its applications* (Vol. 2). New York: Wiley.
- Fisher, R. A. (1922). On the mathematical foundations of theoretical statistics. *The Philosophical Transactions of the Royal Society*, 222, 309-368.
- Fridlund, A. J., & Cacioppo, J. T. (1986). Guidelines for human electromyographic recording. *Psychophysiology*, 23, 567-589.
- Goldstein, I. B. (1972). Electromyography: A measure of skeletal muscle response. In N. S. Greenfield & R. A. Sternbach (Eds.), *Handbook of psychophysiology* (pp. 329-366). New York: Holt, Rinehart & Winston.
- Grabner, M., Andonian, M., Regnier, M., & Harding, V. (1984, May). *Topographical analysis of surface EMG before and after isometrically induced fatigue*. Paper presented at the American College of Sports Medicine Annual Meeting, San Diego, CA.
- Granger, C. W. J. (1966). The typical spectral shape of an economic variable. *Econometrica*, 34, 150-161.
- Hildebrand, D. K. (1971). Kurtosis measures bimodality? *The American Statistician*, 25(1), 42-43.
- Hjorth, B. (1970). EEG analysis based on time domain properties. *Electroencephalography and Clinical Neurophysiology*, 29, 306-310.
- Hjorth, B. (1973). The physical significance of time domain descriptors in EEG analysis. *Electroencephalography and Clinical Neurophysiology*, 34, 321-325.
- Hjorth, B. (1975). Time domain descriptors and their relation to a particular model for generation of EEG activity. In G. Dolce & H. Kunkel (Eds.), *CEAN: Computerized EEG analysis* (pp. 3-8). Stuttgart, FRG: Gustav Fischer Verlag.
- Hoel, P. G., Port, S. C., & Stone, S. J. (1971). *Introduction to probability theory*. Boston: Houghton Mifflin.
- Johnson, N. L., & Kotz, S. (1970). *Continuous univariate distributions—1: Distributions in statistics*. New York: Wiley.
- Kendall, M. G., & Stuart, A. (1963). *The advanced theory of statistics*: (Vol. 1). London: Hafner.
- Lippold, O. C. J. (1967). Electromyography. In P. H. Venables & I. Martin (Eds.), *Manual of psychophysiological methods* (pp. 245-298). New York: Wiley.
- Lord, F. M. (1952). A theory of test scores. *Psychometric Monographs*, Whole No. 7.
- Lykken, D. T., Tellegen, A., & Thorkelson, K. (1974). Genetic determination of EEG frequency spectra. *Biological Psychology*, 1, 245-259.
- McGuigan, F. J. (1978). *Cognitive psychophysiology: Principles of covert behavior*. Englewood Cliffs, NJ: Prentice-Hall.
- Moors, J. J. A. (1986). The meaning of kurtosis: Darlington reexamined. *The American Statistician*, 40(4), 283-284.
- Mosteller, F., & Tukey, J. W. (1968). Data analysis including statistics. In G. Lindzey & E. Aronson (Eds.), *Handbook of social psychology* (Vol. 2, pp. 80-203). Reading, MA: Addison-Wesley.
- Norton, R. M., & Arnold, S. (1985). A theorem on moments. *The American Statistician*, 39(2), 106.
- Peatman, J. G. (1947). *Descriptive and sampling statistics*. New York: Harper and Brothers.
- Passon, A., & Hjorth, B. (1983). EEG topogram—An aid in describing EEG to the clinician. *Electroencephalography and Clinical Neurophysiology*, 56, 399-405.
- Rao, C. R. (1965). *Linear statistical inference and its applications*. New York: Wiley.
- Rey, W. J. J. (1978). *Robust statistical methods*. New York: Springer-Verlag.
- Saltzberg, B. (1973). Period analysis. In A. Remond (Ed.), *Handbook of Electroencephalography and Clinical Neurophysiology* (Vol. 5a, pp. 67-78). Amsterdam: Elsevier.
- Saltzberg, B., & Burch, N. R. (1971). Period analytic estimates of moments of the power spectrum: A simplified EEG time domain procedure. *Electroencephalography and Clinical Neurophysiology*, 30, 568-570.
- Saltzberg, B., Burton, W. D., Jr., Barlow, J. S., & Burch, N. R. (1985). Moments of the power spectral density estimated from samples of the autocorrelation function—a robust procedure for monitoring changes in the statistical properties of lengthy non-stationary time series such as the EEG. *Electroencephalography and Clinical Neurophysiology*, 61, 89-93.
- Saunders, M. G. (1963). Amplitude probability density studies on alpha and alpha-like patterns. *Electroencephalography and Clinical Neurophysiology*, 15, 761-767.
- Saunders, M. G. (1972). The genesis of the EEG. *International Review of Neurobiology*, 15, 227-272.
- Spehr, W., Sartorius, H., Berglund, K., Hjorth, B., Kablitz, C., Plog, V., Wiedemann, P. H., & Zapf, K. (1977). EEG and haemodialysis. A structural survey of EEG spectral analysis. Hjorth's EEG descriptors, blood variables and psychological data. *Electroencephalography and Clinical Neurophysiology*, 43, 787-797.
- Tukey, J. W. (1969). Analyzing data: Sanctification or detective work? *American Psychologist*, 24, 83-91.

Received January 23, 1986

Revision received February 23, 1987

Accepted April 28, 1987 ■